

Potential calculation for alkaline-earth-metal-ion—rare-gas-atom pairs and its application to line-core analysis

H. Harima, T. Ihara,* Y. Urano, and K. Tachibana

Department of Electronics, Kyoto Institute of Technology, Matsugasaki, Kyoto 606, Japan

(Received 5 May 1986)

The pseudopotential model of Baylis has been applied to alkaline-earth-metal (singly ionized)—rare-gas-atom pairs to calculate adiabatic potentials for some low-lying states. Using the calculated potentials, broadening and shift rates of resonance lines of Sr^+ , Ca^+ , and Mg^+ perturbed by Ar and He have been calculated and compared with experiments. The overall agreement is good.

I. INTRODUCTION

Although ionic alkaline-earth-metal spectral lines show important features in solar and stellar spectra, data of their collision broadening by rare gases are scarce compared with, e.g., neutral-alkali-metal—rare-gas pairs.¹ In addition, the agreement between existing line-core data and theoretical calculations is not necessarily good.^{2,3} This is mainly due to the lack of reliable interaction potentials between the colliding pairs. In this work we calculate adiabatic potentials for some low molecular states for the pairs; then to discuss their validity, we evaluate the broadening and shift rates of some resonance lines of the alkaline-earth-metal ion (hereafter abbreviated as AE ion) perturbed by rare gases (abbreviated as RG) to compare with published data^{3–6} or with our latest experiment.⁷ In this work we consider Sr^+ , Ca^+ , and Mg^+ for the AE ion, and Ar and He for RG.

Since singly ionized AE elements have the isoelectronic structure of neutral alkali metals, we can conveniently employ the pseudopotential model of Baylis^{8,9} originally applied to alkali-metal—RG pairs with a slight modification. The point is to replace the net charge of the alkali-metal core ($+e$) by that of the AE ion core ($+2e$). In his model the colliding system consists of three bodies: the valence electron of the alkali metal, the alkali-metal core, and the RG atom. The collisional interaction is separated into two parts: an electrostatic interaction acting on these three bodies and a repulsive interaction described by the Gombás-type statistical pseudopotential.¹⁰ The latter part, acting on the electron—RG-atom and alkali-metal-core—RG-atom pairs, replaces the antisymmetrization procedure of the total wave functions of the system and simulates the “Pauli repulsion” at short-range internuclear distance.

His calculation has been refined by many authors for alkali-metal—RG pairs,^{11–13} extended to more complicated systems with two valence electrons,¹⁴ and is now recognized¹ as a convenient method, when correctly applied, to replace accurate yet usually very costly *ab initio* calculations.¹⁵ However, as an exceptional case, it is worth noting here that in alkali-metal—He pairs the Baylis model has been recognized to fail in correctly describing short-

range interactions.^{16,17} Valiron *et al.*¹⁸ have shown that the repulsive interaction between valence electrons and light RG atoms should include an l -dependent (or nonlocal) term to ensure the orthogonality condition between the valence-electron's wave function and RG orbitals. Pascale¹⁹ has greatly improved his previous calculation for alkali-metal—He pairs¹¹ by applying the l -dependent pseudopotential interaction. Since the original model of Baylis is used in this work, we may find a similar defect for AE-ion—He pairs. This point will be further discussed in our analysis.

Previous theoretical work on broadening for AE-ion resonance lines could be reviewed as follows. Hammond⁴ and Bowman and Lewis⁶ considered Ca^+ lines perturbed by He and Ar by a classical method based on the van der Waals interaction and compared them with their experiments. The observed values are about 1.3 to 2 times larger than their calculations. Giusti-Suzor and Roueff² considered Ca^+ and Sr^+ perturbed by He by a semiclassical method. Their potential model is called the exchange interaction, where a Fermi-type repulsive interaction²⁰ between the valence electron and RG atom is considered. They also report that Hammond's data are larger than their prediction by a factor of 1.4. Bottcher *et al.*²¹ made a quantum-mechanical calculation of the Mg^+ -He interaction. They used a model potential method, where the colliding system is treated as three bodies as in the Baylis model. However, the interactions for these three bodies are described by complicated model functions involving several empirical parameters. More importantly, the wave functions are prepared in antisymmetrized form, so that we do not need terms such as Gombás-type pseudopotential to simulate the Pauli repulsion. Unfortunately their calculations²¹ have not yet been compared with experiments. Therefore we will do that later.

Conventionally the Ca^+ resonance lines corresponding to transitions ${}^2P_{1/2}$ - ${}^2S_{1/2}$ and ${}^2P_{3/2}$ - ${}^2S_{1/2}$ are referred to as the H and K lines, respectively, by the Fraunhofer nomenclature. Therefore, in this paper we shall for convenience use this nomenclature for the analogous lines of Mg^+ and Sr^+ . In Sec. II the potential calculation is described, and in Sec. III the line-core broadenings are calculated and compared with experimental data.

II. POTENTIAL CALCULATION

A. Method

The details of the pseudopotential model are described in the original paper of Baylis,⁸ and the outline was repeatedly described by many authors such as Pascale and Vandeplanque.¹¹ Therefore in this section we give only the key points emphasizing the modification for the present colliding pairs from alkali-metal-RG pairs.

We assume both the AE-ion core and RG atom are represented by undisturbed electronic wave functions during collisions, i.e., they are "frozen." This seems to be a reasonable assumption in usual thermal collisions. Then the problem reduces to finding the eigenvalues of the Hamiltonian

$$H(\mathbf{r}, \mathbf{R}) = H_A(\mathbf{r}) + V(\mathbf{r}, \mathbf{R}). \quad (1)$$

Here \mathbf{r} and \mathbf{R} are the position vectors of the valence electron and of the RG atom, respectively, relative to the AE-ion core. $V(\mathbf{r}, \mathbf{R})$ describes the collisional interaction. When R is infinity it vanishes and $H(\mathbf{r}, \mathbf{R})$ reduces to $H_A(\mathbf{r})$, the Hamiltonian of the free ion.

$V(\mathbf{r}, \mathbf{R})$ consists of three parts

$$V(\mathbf{r}, \mathbf{R}) = F(\mathbf{r}, \mathbf{R}) + G(\mathbf{r}, \mathbf{R}) + W(R), \quad (2)$$

where $G(\mathbf{r}, \mathbf{R})$ and $W(R)$ are the Gombás-type pseudopotential¹⁰ which represents the Pauli repulsion between the valence electron and RG atom, and ion core and RG atom, respectively. $F(\mathbf{r}, \mathbf{R})$ is the electrostatic interaction for the three bodies written as

$$F(\mathbf{r}, \mathbf{R}) = -\frac{\alpha}{2} \left[\frac{2e\mathbf{R}}{R^3} + \frac{e\mathbf{r}'}{r'^3} \right]^2. \quad (3)$$

Here α is the electric dipole polarizability of the RG, e is the elementary charge, and $\mathbf{r}' = \mathbf{r} - \mathbf{R}$. In alkali-metal-RG collisions the net charge of the alkali-metal core is $+e$ instead of $+2e$, thus the term $2e\mathbf{R}/R^3$ is replaced by $e\mathbf{R}/R^3$. As done by Baylis⁸ we define an effective radius r_0 for the RG atom, and if $r' < r_0$ (3) can be replaced by

$$F(\mathbf{r}, \mathbf{R}) = -\frac{\alpha}{2} \left[\frac{4e^2}{R^4} + \frac{4e^2}{r_0^4} \right]. \quad (4)$$

When $r' > r_0$ (3) must be directly calculated. Baylis determined r_0 by fitting the well depth of the calculated ground-state potential to that obtained from scattering experiments. Unfortunately for AE-ion-RG-atom pairs we have no such data. Therefore, in this work we employ the values of Baylis⁸ for alkali-metal-RG pairs which have the same electronic configurations. For example, for the Sr^+ -Ar pair we write $r_0 = 1.063$ a.u. as assumed for Rb-Ar (1 a.u. = 0.53 Å). We will check later how sensitive the calculated potentials are to the magnitude of r_0 .

To calculate $G(\mathbf{r}, \mathbf{R})$ and $W(R)$ we must know the charge distributions of the outermost shells of the RG, $\rho_B(r)$, and of AE-ion core $\rho_A(r)$. They were taken from Gombás¹⁰ and Gombás and Szondy,²² respectively. The exact calculation of $G(\mathbf{r}, \mathbf{R})$ and $W(R)$ is very time consuming on the computer. Therefore we have evaluated

these terms by the same approximation as described by Baylis.⁸

As the basis set used to diagonalize $H(\mathbf{r}, \mathbf{R})$ in (1), Baylis employed the eight lowest states of the alkali-metal atom which form the lowest $^2S_{1/2}$, $^2P_{1/2}$, and $^2P_{3/2}$ levels. Such a limitation of the basis set is one of the important assumptions in his method. This seems reasonable when only low molecular states are concerned.¹¹ In the present case, Sr^+ and Ca^+ have the first $^2D_{3/2,5/2}$ levels lying between the ground $^2S_{1/2}$ and the first $^2P_{1/2,3/2}$ levels, and there is a large energy defect between the first 2P levels and the next upper level (the second 2S level). In Mg^+ both the first 2D and the second 2S levels are much higher than the first $^2P_{1/2,3/2}$ levels. Therefore, for Ca^+ and Sr^+ we considered ten states belonging to $^2D_{3/2,5/2}$ in addition to the above eight states. The radial part of the wave functions for these states are given by the Bates-Damgaard type²³ as was done by Baylis.

B. Results

In addition to r_0 , we need the following parameters in computation: the energy levels of AE ions and dipole polarizabilities of the RG. They were taken respectively from Moore²⁴ and Dalgarno and Kingston.²⁵ In the following we will give first the general characteristics of the calculated potential shape, then compare with other calculations and potentials for alkali-metal-RG pairs with isoelectronic configurations, and finally discuss the sensitivity of potential shape to r_0 .

Figures 1–3 show the calculated adiabatic potentials. As the internuclear separation R increases, the potential curves approach the corresponding atomic limits. These asymptotes are marked on the right-hand side of each figure. Each potential curve is specified by $\Omega (= |m_j|) = \frac{1}{2}, \dots$, where m_j is the projection of total angular momentum of the valence electron along the in-

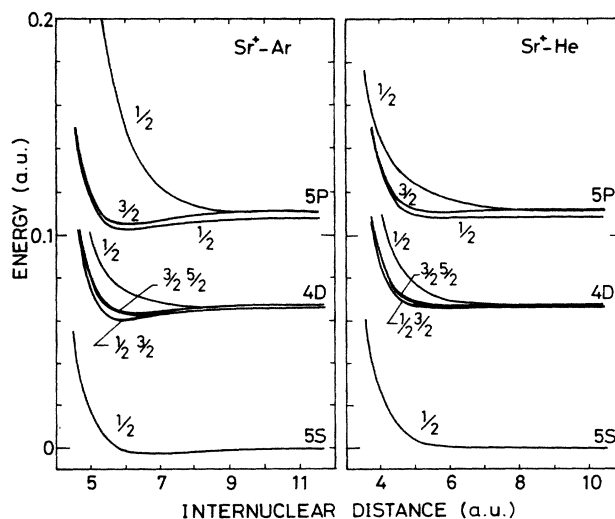


FIG. 1. Adiabatic potentials for Sr^+ rare-gas pairs with $r_0 = 1.063$ for Ar and 0.685 a.u. for He. 1 a.u. = 2.19×10^5 cm⁻¹.

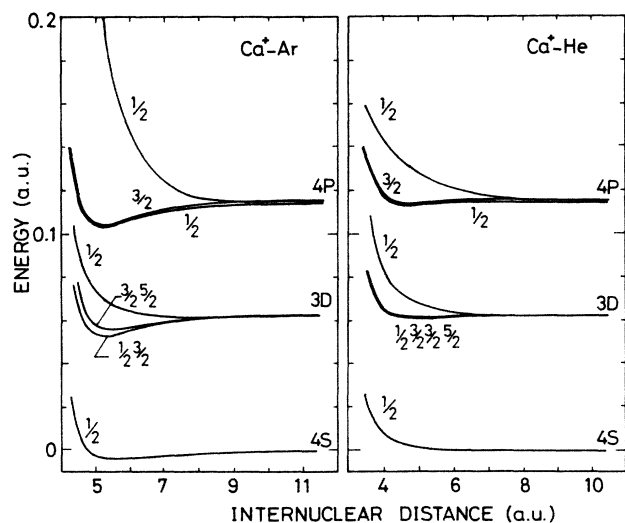


FIG. 2. Adiabatic potentials for Ca^+ rare-gas pairs with $r_0 = 1.091$ for Ar and 0.704 a.u. for He.

ternuclear axis. For a given AE ion, the potential wells in various states become pronounced for the heavier RG, Ar, than the lighter one, He. This can be explained by the difference of dipole polarizabilities of RG as calculated for alkali-metal-RG pairs.^{8,11} The depth ϵ and position R_m of each potential well are determined by the balance of the long-range attractive interaction $F(\mathbf{r}, \mathbf{R})$ and the short-range repulsive terms $G(\mathbf{r}, \mathbf{R})$ and $W(R)$. The attractive term is proportional to the polarizabilities α as shown in (3), while the repulsive terms do not show such a drastic change with the RG species in the present R region. The well positions related to S and P asymptotes are summarized in Table I. Here the molecular states are labeled as $X^2\Sigma_{1/2}$, $A^2\Pi_{1/2,3/2}$ and $B^2\Sigma_{1/2}$ following Herzberg notation. Since we are mainly concerned with P - S optical transitions, molecular states related to D asymptotes are not discussed in the following. For a given RG the wells become deeper as one goes from heavier to light AE ions. This may be understood by the difference of the above repulsive interaction. The term $G(\mathbf{r}, \mathbf{R})$ which describes the Pauli repulsion between the valence electron and the RG is sensitive to the spread of valence-electron clouds. As an example we compare

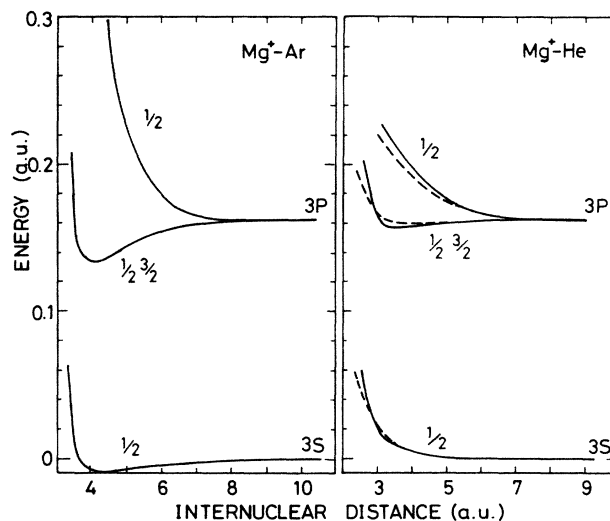


FIG. 3. Adiabatic potentials for Mg^+ rare-gas pairs with $r_0 = 1.210$ for Ar and 0.866 a.u. for He (—). Calculation of Bottcher *et al.* (Ref. 21) is shown for comparison (---).

charge distributions of valence electrons of Sr^+ and Mg^+ in s and p orbitals in Fig. 4. We find that the clouds of Sr^+ spread outward more than in Mg^+ . Therefore, as R decreases the term $G(\mathbf{r}, \mathbf{R})$ begins to act at larger values of R for Sr^+ than for Mg^+ .

Next we compare our system with alkali-metal-RG pairs having the same electronic configurations. Since we observe a similar tendency, we discuss the Sr^+ -Ar pair again to compare with Rb-Ar. The well parameters for the Rb-Ar pair determined by Baylis⁸ are shown in the last row of Table I. We see the Sr^+ -Ar pair has much (about 5 to 13 times) deeper wells at shorter internuclear distance than the Rb-Ar pair. This may be explained as follows. First, Rb has valence-electron clouds which spread outward much more than Sr^+ as are clearly seen in Fig. 4. Thus the term $G(\mathbf{r}, \mathbf{R})$ begins to act at very large values of R for Rb compared with Sr^+ . Second, in the Sr^+ -Ar pair the long-range attractive interaction is dominated by the strong polarization force written as $-e^2R^{-4}/2$, which acts between a point charge of e and an induced dipole. In the Rb-Ar pair, however, the dominant term is the weak van der Waals attraction with R^{-6}

TABLE I. Well positions (R_m, ϵ) related to $^2S_{1/2}$, $^2P_{1/2}$, and $^2P_{3/2}$ states. They are given in a.u. for R_m and cm^{-1} for ϵ .

	$X^2\Sigma_{1/2}$	$A^2\Pi_{1/2}$	$A^2\Pi_{3/2}$	$B^2\Sigma_{1/2}$
Mg^+ -He	(6.2,96)	(3.6,1152)	(3.6,1182)	(8.7,28)
Mg^+ -Ar	(4.1,2310)	(4.0,6555)	(4.0,6585)	(8.4,269)
Ca^+ -He	(7.2,58)	(4.8,371)	(4.8,443)	(9.7,20)
Ca^+ -Ar	(5.5,836)	(5.2,2718)	(5.2,2794)	(9.4,192)
Sr^+ -He	(7.6,48)	(9.0,24)	(5.8,217)	(10.3,16)
Sr^+ -Ar	(6.6,575)	(6.0,1283)	(5.9,1560)	(9.8,163)
Rb-Ar ^a	(9.9,43.5)	(6.8,238)	(6.8,315)	(15.6,11.9)

^aReference 8.

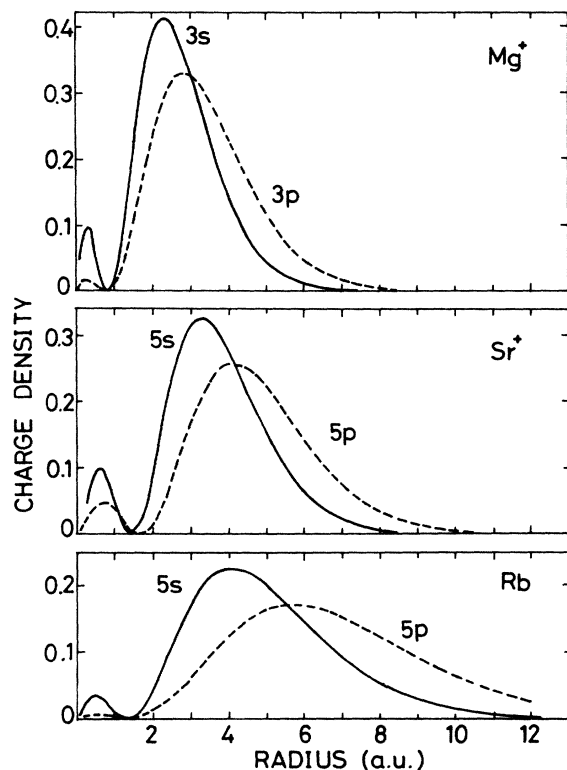


FIG. 4. Charge distributions of valence electron. Charge density is defined by the square of Bates-Damgaard-type wave functions.

dependence between two induced dipoles. As shown in the Appendix, we can easily show by expanding $F(r, R)$ in infinite power series of r/R that $F(r, R)$ for the AE-ion-RG pair is actually dominated by the above polarization force at large R . This is graphically shown in Fig. 5.

As described in the Introduction, only limited calculations are reported for the AE-ion-RG pair potentials. Among them, we believe, the result of Bottcher *et al.*²¹ for the $Mg^+ - He$ pair is most sophisticated. Since their result is shown only graphically, we will replot them in Fig. 3 by dashed curves to compare with ours. We find both results have similar behavior, e.g., the uppermost state with $\Omega = \frac{1}{2}$ gradually increases repulsive character as R decreases, while the other potentials steeply rise at $R \lesssim 3$ a.u. However, there are some distinct differences: (i) potentials of Bottcher *et al.* are all less repulsive at small R (< 3 a.u.) values, and (ii) the lower excited states ($\bar{\Omega} = \frac{1}{2}, \frac{3}{2}$) of $3P$ asymptotes have wells of depth ~ 1000 cm^{-1} at $R = 3.6$ a.u. in our calculation (Table I), while in the result of Bottcher *et al.* the potentials are almost flat at $R \gtrsim 3$ a.u. As for (i), Bottcher *et al.*²⁶ reports similar discrepancy from Baylis potential for alkali-metal (Li, Na) - RG (He, Ne) pairs. In the present Baylis model calculation the core-core repulsion term $W(R)$ plays the most important role in such a small- R region. As discussed by Valiron *et al.*,^{16,18} this difference may be attributed to the lack of a corresponding term in the model Hamiltonian of Bottcher *et al.* [Eq. (5) of Ref. 21].

Finally, we discuss how the potential shape is influ-

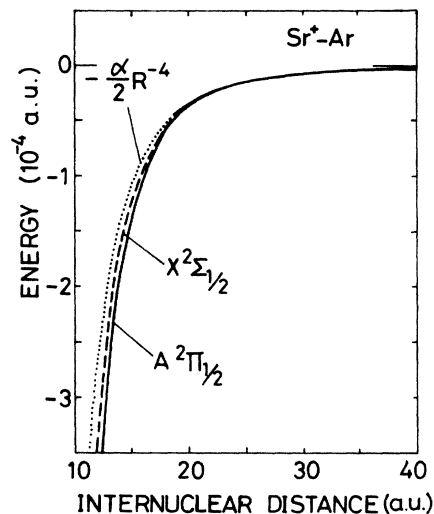


FIG. 5. Long-range potentials for $Sr^+ - Ar$ pair. At $R \geq 20$ a.u. they are well described by the polarization force. Other states (${}^2\Pi_{3/2}, {}^2\Sigma_{1/2}$) behave similarly.

enced by the magnitude of r_0 . It gives a measure of the spread of charge distribution of the RG. Thus one may expect that the assumption of r_0 may severely affect the terms $G(r, R)$ and $F(r, R)$ in the relatively small- R region. In changing r_0 , however, we have at present no definite base to estimate a "reasonable" range of r_0 . Obviously r_0 should increase with the mass of the RG. As a test case we increased r_0 for the $Sr^+ - Ar$ pair from 1.063 to 1.186. This latter value was used by Baylis for the Rb-Kr pair.⁸ Thus it may be looked at as a rough estimate of the upper limit for the $Sr^+ - Ar$ pair. The comparison is shown in Fig. 6. The Σ states are more repulsive for the larger r_0 , while the Π states show no discernible effect. This is ex-

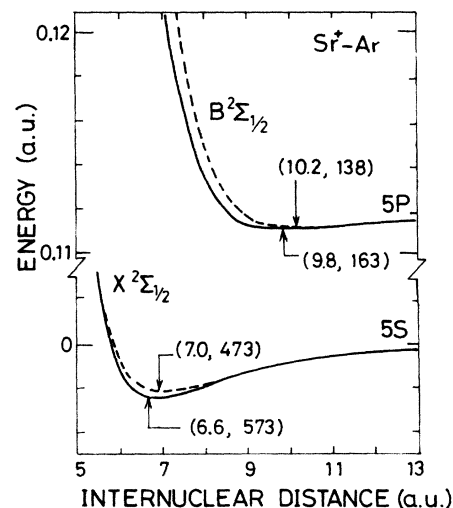


FIG. 6. r_0 dependence for $Sr^+ - Ar$ pair (—, $r_0 = 1.063$; ---, $r_0 = 1.186$ a.u.). Respective well parameters (R_m, ϵ) are shown with R_m in a.u. and ϵ in cm^{-1} . Π states are not shown because they show no discernible change on this scale.

plained by the charge distribution of the valence electron. In the $B^2\Sigma_{1/2}$ state it spreads along the internuclear axis, therefore the repulsive character is enhanced for the larger r_0 . In the $A^2\Pi_{1/2,3/2}$ states, however, it spreads vertically against the internuclear axis, thus the effect is negligible. For the $X^2\Sigma_{1/2}$ state the effect is somewhat weaker than for the $B^2\Sigma_{1/2}$ state. As one changes r_0 from 1.063 by 10%, the well depth of Σ states changes by about 20%. When the perturber is He, the effect is somewhat larger.

III. BROADENING CALCULATION

A. Method

In this section we consider the line-core broadening and shift of AE-ion resonance lines in a semiclassical treatment of the impact approximation. We will mainly discuss H lines, since they can be treated somewhat more easily than K lines.

If the perturber density is low and collisions have short durations, the spectral line shape takes the Lorentzian form

$$I(\omega) \propto 1/[(\omega_0 - \omega + \beta)^2 + \gamma^2]. \quad (5)$$

The width γ and shift β are given by

$$\gamma + i\beta = 2\pi n \int_0^\infty f(v)v dv \int_0^\infty [1 - \Pi(\rho, v)] \rho d\rho, \quad (6)$$

where n is the perturber density, v is the relative velocity, $f(v)$ is its distribution function, and ρ is the impact parameter. In our calculation the averaging over velocity in (6) was replaced by taking its mean value \bar{v} . The resulting error should be negligible.²⁷ In our case, perturbers (RG) remain in the ground S state during collisions, therefore $\Pi(\rho, v)$ is described as²⁸

$$\begin{aligned} \Pi(\rho, v) = \sum_{m_i, m_f} \begin{pmatrix} j_f & 1 & j_i \\ m_f & M & -m_i \end{pmatrix}^2 \langle j_i m_i | S | j_i m_i \rangle \\ \times \langle j_f m_f | S^{-1} | j_f m_f \rangle. \end{aligned} \quad (7)$$

Here $|j_f, m_f\rangle$ and $|j_i, m_i\rangle$ denote the ground and excited states of the AE ion, respectively. S is the scattering matrix defined by the wave functions in the interaction representation before and after a collision by

$$\psi(t = +\infty) = S\psi(t = -\infty). \quad (8)$$

We will write the interaction Hamiltonian of the system in a matrix form taking eight atomic basis sets $|^2S_{1/2}, \pm\frac{1}{2}\rangle$, $|^2P_{3/2}, \pm\frac{3}{2}\rangle$, $|^2P_{3/2}, \pm\frac{1}{2}\rangle$, and $|^2P_{1/2}, \pm\frac{1}{2}\rangle$, with the quantization axis along \mathbf{R} (rotating frame). Then ψ is expressed in a 1×8 column vector $|\mathbf{a}\rangle$ of coupling coefficients (closed-coupled treatment). If we assume there is no coupling between the ground and excited states, the Hamiltonian is decoupled to a 2×2 matrix for the ground state, and a 6×6 matrix for the excited states. The explicit form for the latter is given, e.g., by Allard and Kielkopf.¹ If the coupling term between $|^2P_{3/2}, \pm\frac{1}{2}\rangle$ and $|^2P_{1/2}, \pm\frac{1}{2}\rangle$ states (i.e., fine-structure

mixing) is ignored, then this matrix is further decoupled to a 2×2 matrix corresponding to $^2P_{1/2}$, and a 4×4 matrix corresponding to $^2P_{3/2}$ states. The former one could be written as

$$\begin{pmatrix} V(\Pi_{1/2}) & iV_R \\ -iV_R & V(\Pi_{1/2}) \end{pmatrix}. \quad (9)$$

Here $V(\Pi_{1/2})$ is the molecular perturbation for the $^2\Pi_{1/2}$ state. Since we choose a rotating frame, rotational coupling V_R appears in the nondiagonal term. If such simplifications are unacceptable, we must solve the problem rigorously. In the present calculation we employed the formalism of Roueff *et al.*^{29,30} This is because we want to compare our results with their calculations² for Ca^+ and Sr^+ following the same procedure. Strictly speaking, there is a slight difference from that of the Baylis model⁸ in the treatment of spin-orbit interaction in the Hamiltonian. But it would not cause a serious problem in the present calculation as confirmed previously for Rb-RG pairs.³⁰ In the actual calculation of the time evolution of the column vector from $t = -\infty$ to $+\infty$ we assign, instead of infinity, $t_{\max} = R_{\max}/\bar{v}$ as the maximum of time, where $R_{\max} = 40$ a.u. for Ar and 30 a.u. for He. Differential equations of coupling coefficients were solved numerically by a Runge-Kutta algorithm along the following perturber trajectories. If the interaction Hamiltonian related to the $^2P_{1/2}$ state is decoupled to a 2×2 matrix such as (9), we have only to consider the $^2\Pi_{1/2}$ potential to calculate the broadening of H line. Thus the trajectory is uniquely determined by the classical law of energy conservation as

$$dR/dt = \pm \bar{v} \{1 - \rho^2/R^2 - V[\Pi_{1/2}(R)]/E\}^{1/2}, \quad (10)$$

where E is the initial kinetic energy, and the term $-V[\Pi_{1/2}(R)]/E$ describes the trajectory deflection. If the Hamiltonian is not decoupled, the trajectory is not uniquely determined. In this case we assume straight trajectories. From (10) we see this is valid when E is large compared with the collisional perturbation (high-energy limit). Therefore slow and close collisions are not accurately treated in this method. We will hereafter call the former method the "simple treatment" and the latter the "rigorous treatment."

B. Results

In Table II calculated results are shown and compared with experiments. For the H line in the Mg^+ -He pair we have no experimental data, thus the K line is compared instead. In our calculations suitable treatment, simple or rigorous, was used depending on the fine-structure separation $\Delta\omega$ between nearby molecular states and temperature T . At low temperature with large $\Delta\omega$ the simple treatment is suitable, because the adiabatic criterion $\hbar/\tau_c \ll \Delta\omega$ is satisfied (τ_c is the collision duration). Then we can ignore the fine-structure mixing. Let us compare the Sr^+ -Ar pair with Mg^+ -Ar, for example. In both cases \hbar/τ_c is roughly 4×10^{-4} a.u. at $T \simeq 700$ K, if we estimate it as $\tau_c \simeq \rho/\bar{v}$ with $\rho = 10$ a.u. Thus for the Sr^+ -Ar pair ($\Delta\omega \sim 3 \times 10^{-3}$ a.u.) this criterion is satisfied, but not for the Mg^+ -Ar pair ($\Delta\omega \sim 4 \times 10^{-4}$ a.u.).

First we confirmed that there was no systematic error in our computation. Giusti-Suzor and Roueff² calculate broadening of Ca^+ and Sr^+ resonance lines perturbed by He at 4500 K by what they call the “complete treatment,” which is equivalent to our rigorous one. Their basic model potential is an exponential repulsion called the exchange interactions²⁰ (abbreviated as EI) between the valence electron in the Σ states and RG atom. The EI have rather simple analytic forms and are given in the paper.² By putting them into our computer code of rigorous treatment we have precisely reproduced their value.

By looking at Table II we find the overall agreement is reasonably good, though there are some exceptions such as $2\gamma/n$ for the Ca^+ -Ar pair at 875 K. We would like to emphasize that previous large discrepancies between theory and experiment, especially at high temperatures, are greatly improved by our calculation. Let us discuss $2\gamma/n$ for the Ca^+ -He pair at 5200 K, for example. Previously, Bowman and Lewis⁶ calculated it classically by the conventional van der Waals approximation.³¹ ($2\gamma/n = 1.99$ in the unit of $10^{-20} \text{ cm}^{-1}/\text{cm}^{-3}$. This unit will be used below for broadening and shift rates.) They also extrapolated the values of Giusti-Suzor and Roueff²

to 5200 K ($2\gamma/n = 1.74$). Calculating accurately with the EI model² we get the value of 1.81. All these values are too small compared with the experimental result of Hammond ($2\gamma/n = 2.56$).⁴ But when the model potential is replaced by ours we obtain fairly good agreement ($2\gamma/n = 2.43$). In Fig. 7(a) we can see clearly why the EI model yields such a small value. Here the real part of $[1 - \Pi(\rho, \bar{v})]\rho$, the integrand appearing in (6), is compared with our potential and the EI model. Obviously these two curves behave in a quite different manner at $5 < \rho < 7$ a.u. This difference could be well understood if we look at Fig. 8 where the EI model is compared with our potential. The EI model well simulates the $X^2\Sigma_{1/2}$ state at $R \gtrsim 5$ a.u., but for the excited states our potentials behave more drastically than the EI model at $R \lesssim 7$ a.u. If we discuss the classical phase-shift theory,³² such a drastic change increases the phase change in each collision yielding a large broadening rate. In the imaginary part shown in Fig. 7(b) the difference at $5 < \rho < 8$ a.u. is striking again. In our potential the large negative contribution gives negative shift ($\beta/n = -0.22$), while in the EI model it is positive ($\beta/n = 0.20$). If we refer to the observed shift rate at 655 K ($\beta/n = -0.19$), the negative sign would be realistic.

TABLE II. Broadening and shift rates for the H-line ($^2P_{1/2} - ^2S_{1/2}$) perturbed by Ar and He ($10^{-20} \text{ cm}^{-1}/\text{cm}^{-3}$). Fine-structure separation $\Delta\omega$ of 2P state for isolated ion is given in cm^{-1} and a.u.

$\Delta\omega$	Calculation		Experiment		Temperature (K)
	$2\gamma/n$	β/n	$2\gamma/n$	β/n	
Sr^+ -Ar 801 cm^{-1} (3.7×10^{-3})	1.60 ^a	-0.44 ^a	1.87 ± 0.25^b		690
	1.51 ^a	-0.35 ^a	1.44 ± 0.12^c	-0.20 ± 0.05^c	608
Ca^+ -Ar 223 cm^{-1} (1.0×10^{-3})	1.55 ^a	-0.28 ^a	1.57 ± 0.04^d		765
	1.11 ^e				765
	1.90 ^a	-0.30 ^a	1.24 ± 0.08^e	-0.26 ± 0.05^e	875
	1.99 ^f				875
	2.64 ^f	-0.90 ^f	2.79 ± 0.67^g		7466
	2.20 ^e				7466
Mg^+ -Ar 92 cm^{-1} (4.2×10^{-4})	1.62 ^f	-0.46 ^f	1.14 ± 0.13^e	-0.32 ± 0.17^e	754
Sr^+ -He	0.77 ^a	+0.04 ^a	1.09 ± 0.09^e	$+0.34 \pm 0.04^e$	573
Ca^+ -He	0.89 ^f	-0.11 ^f	1.11 ± 0.06^e	-0.19 ± 0.06^e	655
	2.43 ^f	-0.22 ^f	2.56 ± 0.77^b		5200
	1.81 ⁱ	+0.20 ⁱ			5200
	1.99 ^e				5200
Mg^+ -He	0.79 ^f	-0.15 ^f			556
	1.05 ^j	-0.12 ^j	1.90 ± 0.02^e	-0.39 ± 0.05^e	556

^aPresent calculation (simple treatment with our potential).

^bReference 7.

^cReference 3.

^dReference 6.

^eClassical van der Waals approximation of Bowman and Lewis (Ref. 6). Their value for Ca^+ -Ar pair at 7466 K ($= 1.21$) is probably incorrect. It should be 2.20 if $T^{0.3}$ temperature dependence is assumed.

^fPresent calculation (rigorous treatment with our potential).

^gReference 5.

^hReference 4.

ⁱPresent calculation (rigorous treatment with exchange interaction given in Ref. 2).

^jPresent calculation (rigorous treatment with our potential for K line).

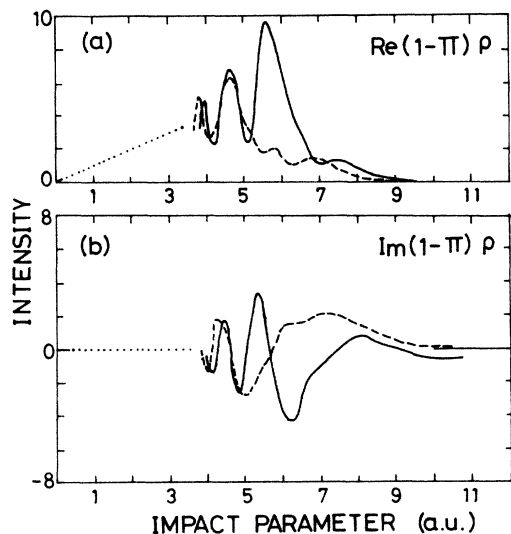


FIG. 7. (a) Real and (b) imaginary part of the integrand in Eq. (6) calculated with our potential (—) and exchange interaction of Ref. 2 (---). When rapid oscillations appear ($\rho \leq 3.5$ a.u.), the mean values ($\cdot \cdot \cdot$) are computed. They have slope of 1 for (a) and 0 for (b).

Therefore, to assess the shift rate correctly, one must add some long-range attractive interaction to EI as suggested by Giusti-Suzor and Roueff.²

Let us discuss finally the large discrepancy observed in Table II. For $2\gamma/n$ of the Ca^+ -Ar pair at 875 K, our calculations based on simple and rigorous treatments are both greater than the experiment by about 50%. This is quite puzzling, because fairly good agreement is obtained at different temperatures. For Ca^+ -He, Sr^+ -He, and Mg^+ -He pairs, serious discrepancy appears in the shift rates. In alkali-metal-He pairs⁸ r_0 is not uniquely deter-

mined, but a certain range of estimation is given. We could not obtain good agreement for the shift rate only by adjusting r_0 within this range. We can obtain better agreement if r_0 greatly exceeds this range, but the value has little physical meaning. In the Mg^+ -He pair the discrepancy for the broadening rate is also apparent. This situation does not change even if we recall the calculation of Bottcher *et al.*²¹ From their figure showing the temperature dependence of broadening rate we can read $2\gamma/n < 1 \times 10^{-20} \text{ cm}^{-1}/\text{cm}^{-3}$ at 556 K. This indicates that the employed potentials should be greatly modified. In our case, we probably have to reconsider various parameters used in the potential calculation such as the selection of the basis set, or core charge distributions. More essentially, we have to check carefully the validity of the potential model itself at relatively small internuclear distance where broadening and shift rates are greatly affected as in the case of the Mg^+ -He pair. It is worth comparing the colliding pair with the isoelectronic system, Na-He. As described in the Introduction, short-range repulsive interaction between the valence electron and the RG atom (especially the lightest ones) is not accurately calculated by l -independent (or local) pseudopotential interaction as used in the Baylis model. For the Na-He pair Hanssen *et al.*¹⁶ and Pascale¹⁹ have shown by sophisticated calculations along this line that previous potential shapes¹¹ should be greatly modified; e.g., the well position of the first $^2\Pi$ state (R_m, ϵ) = (6.2 a.u., 32 cm^{-1})¹¹ should be replaced by (4.35 a.u., 511 cm^{-1}).¹⁹ Line-core data are generally not so sensitive to very short-range interactions as far-wing spectra as demonstrated by these authors, however, such a drastic change of potential shapes may severely affect also the core data. Although we did not try such sophisticated calculations in the present work, the same attempt is obviously a future direction to improve the accuracy of potentials for AE-ion-He pairs.

IV. CONCLUSIONS

By applying the Baylis model potential to alkaline-earth-metal (singly ionized)-rare-gas-atom pairs, we calculated interaction potentials for some low molecular states. Although they have certain uncertainty coming from some unknown parameters, we can reasonably explain most of the observed broadening data of resonance lines of alkaline-earth-metal ions using these potentials. As a future subject the improvement of potentials for light rare gases should be studied. To extend broadening experiments from the line core to the wing region is also a very interesting topic, from which we can discuss relatively short-range interactions precisely. The latter subject is now in progress in our laboratory, and the first report for the Sr^+ -Ar pair would appear shortly.⁷

ACKNOWLEDGMENT

The authors are very grateful to S. Izeki, K. Yoshimura, K. Kunijima, and K. Harada for helping with the computation.

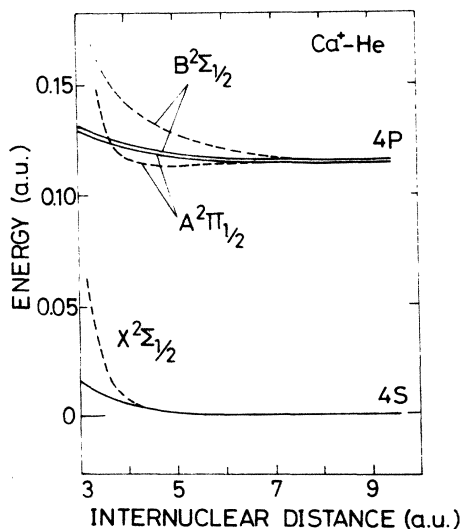


FIG. 8. Comparison of Ca^+ -He potential between our result (---) and exchange interaction (—). In the latter model, the $^2\Pi_{3/2}$ state gets no perturbation (see Fig. 2 of Ref. 2).

APPENDIX

In this section we consider the long-range behavior of $F(\mathbf{r}, \mathbf{R})$. We first follow Baylis's formulas for alkali-metal-rare-gas pairs. In his case the electrostatic interaction

$$F(\mathbf{r}, \mathbf{R}) = -\frac{\alpha}{2} \left[\kappa \frac{e\mathbf{R}}{R^3} + \frac{e\mathbf{r}'}{r'^3} \right]^2 \quad (\kappa=1) \quad (\text{A1})$$

is expanded by Legendre polynomials $P_L(\cos\theta)$, where θ is the angle determined by \mathbf{r} and \mathbf{R} . The long-range behavior of $F(\mathbf{r}, \mathbf{R})$ is determined by its expansion coefficients [see Eq. (A12a) of Baylis⁸]

$$F^{(L)}(r, R) = -\frac{\alpha e^2}{2} \left[\kappa^2 \frac{\delta_{L0}}{R^4} + \frac{a_L(x)}{(R^2 - r^2)^2} - \frac{3}{4} \frac{b_L(x)}{R^2 r^2} \ln \left| \frac{R+r}{R-r} \right| - \kappa \frac{2(L+1)}{R^4} \left[\frac{r}{R} \right]^L \right], \quad (\text{A2})$$

where $\delta_{L0}=1$ only for $L=0$, $x=(R^2+r^2)/2Rr$, and the functions $a_L(x)$ and $b_L(x)$ are tabulated (Table AI of Baylis⁸). For $L=0$ and 2, $a_0(x)=1$, $a_2(x)=5(3x^2-2)$, $b_0(x)=0$, and $b_2(x)=5x$, so that

$$F^{(0)}(r, R) = -\frac{\alpha e^2}{2} \left[\frac{1}{(R^2 - r^2)^2} + \frac{\kappa^2 - 2\kappa}{R^4} \right], \quad (\text{A3})$$

$$F^{(2)}(r, R) = -\frac{\alpha e^2}{2} \left[\frac{5(3x^2 - 2)}{(R^2 - r^2)^2} - \frac{15}{4} \frac{x}{R^2 r^2} \ln \left| \frac{R+r}{R-r} \right| - \kappa \frac{6r^2}{R^6} \right]. \quad (\text{A4})$$

We can omit the contribution of $F^{(1)}(r, R)$ term, since

$$\langle nlm | F^{(1)}(r, R) P_1(\cos\theta) | nlm \rangle = \langle nl | F^{(1)}(r, R) | nl \rangle \langle lm | \cos\theta | lm \rangle = 0,$$

where $|nlm\rangle$ corresponds to the alkali metal's wave functions. Baylis expanded (A3) and (A4) in a power series of r/R [see Eq. (A14) of Baylis⁸]. Similarly, in our case of alkaline-earth-metal(ion)-RG pairs, we can put $\kappa=2$ to get

$$F^{(0)}(r, R) = -\frac{\alpha e^2}{2R^4} \left[1 + \sum_{m=1}^{\infty} (m+1) \left[\frac{r}{R} \right]^{2m} \right], \quad (\text{A5})$$

$$F^{(2)}(r, R) = -\frac{\alpha e^2 r^2}{R^6} \left[-2 + \sum_{m=1}^{\infty} D_m \left[\frac{r}{R} \right]^{2m} \right], \quad (\text{A6})$$

where

$$D_m = 10 \frac{(m+1)(m+2)(m+3)}{(2m+3)(2m+5)}. \quad (\text{A7})$$

Therefore $F(\mathbf{r}, \mathbf{R})$ can be written as

$$F(r, R) = F^{(0)}(r, R) P_0 + F^{(2)}(r, R) P_2(\cos\theta) + \dots = -\frac{\alpha e^2}{2R^4} - \frac{\alpha e^2 r^2}{R^6} [1 - 2P_2(\cos\theta)] - \frac{\alpha e^2 r^4}{R^8} \left[\frac{3}{2} + \frac{48}{7} P_2(\cos\theta) \right] - \dots \quad (\text{A8})$$

Thus starting from the monopole-dipole interaction term (so called the "polarization force") which behaves as R^{-4} , higher-order terms with R^{-6} , R^{-8} , ... follow in the r/R expansion of $F(\mathbf{r}, \mathbf{R})$.

*Present address: Sumitomo Electric Industries LTD., Itami, Hyogo 664, Japan.

¹N. Allard and J. Kielkopf, *Rev. Mod. Phys.* **54**, 1103 (1982).

²A. Giusti-Suzor and E. Roueff, *J. Phys. B* **8**, 2708 (1975).

³R. G. Giles and E. L. Lewis, *J. Phys. B* **15**, 2871 (1982).

⁴G. L. Hammond, *Astrophys. J.* **196**, 291 (1975). There seems to be confusion in the comparison of his observed width (half width at half maximum) with a theoretical formula given by Eq. (32) of his paper. This latter gives full width at half maximum.

⁵J. F. Baur and J. Cooper, *J. Quant. Spectrosc. Radiat. Transfer* **17**, 311 (1977).

⁶N. J. Bowman and E. L. Lewis, *J. Phys. B* **11**, 1703 (1978).

⁷H. Harima, K. Tachibana, and Y. Urano (unpublished).

⁸W. E. Baylis, *J. Chem. Phys.* **51**, 2665 (1969).

⁹W. E. Baylis, JILA Report No. 100, University of Colorado, 1969 (unpublished).

¹⁰P. Gombás, *Pseudopotentiale* (Springer, New York, 1967).

¹¹J. Pascale and J. Vandepanque, *J. Chem. Phys.* **60**, 2278 (1974).

¹²E. Czuchaj and J. Sienkiewicz, *Z. Naturforsch.* **34a**, 694

(1979).

¹³R. Düren and G. Moritz, *J. Chem. Phys.* **73**, 5155 (1980).

¹⁴E. Czuchaj and J. Sienkiewicz, *J. Phys. B* **17**, 2251 (1984).

¹⁵M. Krauss, P. Maldonado, and A. C. Wahl, *J. Chem. Phys.* **54**, 4944 (1971); R. P. Saxon, R. E. Olson, and B. Liu, *ibid.* **67**, 2692 (1977).

¹⁶J. Hanssen, R. McCarroll, and P. Valiron, *J. Phys. B* **12**, 899 (1979).

¹⁷F. Masnou-Seeuws, *J. Phys. B* **15**, 883 (1982).

¹⁸P. Valiron, R. Gayet, R. McCarroll, F. Masnou-Seeuws, and M. Philippe, *J. Phys. B* **12**, 53 (1979).

¹⁹J. Pascale, *Phys. Rev. A* **26**, 3709 (1982); **28**, 632 (1983).

²⁰E. Roueff, *Astron. Astrophys.* **7**, 4 (1970).

²¹C. Bottcher, K. K. Docken, and A. Dalgarno, *J. Phys. B* **8**, 1756 (1975).

²²P. Gombás and T. Szondy, *Solutions of the Simplified S.C.F. for all Atoms of the Periodic System of Elements from Z=2 to Z=92* (Hilger, London, 1970).

²³D. R. Bates and A. Damgaard, *Philos. Trans. R. Soc. London, Ser. A* **242**, 101 (1949).

²⁴C. E. Moore, *Atomic Energy Levels*, Natl. Bur. Stand. Ref.

- Data Ser., Natl. Bur. Stand. (U.S.) Circ. No. 35 (U.S. GPO, Washington, D.C., 1971), Vols. 1 and 2.
- ²⁵A. Dalgarno and A. E. Kingston, Proc. R. Soc. London, Ser. A **259**, 424 (1961).
- ²⁶C. Bottcher, A. Dalgarno, and E. L. Wright, Phys. Rev. A **7**, 1606 (1973).
- ²⁷A. Gallagher, Phys. Rev. **172**, 88 (1968).
- ²⁸E. L. Lewis, Phys. Rep. **58**, 1 (1980).
- ²⁹E. Roueff, J. Phys. B **5**, L79 (1972).
- ³⁰E. Roueff and A. Suzor, J. Phys. **35**, 727 (1974); E. Roueff and H. Abgrall, *ibid.* **38**, 1485 (1977).
- ³¹L. H. Aller, Astrophys, *The Atmospheres of the Sun and the Stars* (Ronald, New York, 1953).
- ³²W. R. Hindmarsh and J. M. Farr, Prog. Quantum Electron. **2**, 141 (1972).